ADVANCES IN ATMOSPHERIC SCIENCES, VOL. 27, NO. 2, 2010, 427–442

Simulation and Evaluation of Terrestrial Ecosystem NPP with M-SDGVM over Continental China

MAO Jiafu*[1] (毛嘉富), DAN Li[2] (丹 利), WANG Bin[1] (王 斌), and DAI Yongjiu[3] (戴永久)

[1]*State Key Laboratory of Numerical Modeling for Atmospheric Sciences and Geophysical Fluid Dynamics, Institute of Atmospheric Physics, Chinese Academy of Sciences, Beijing* 100029

[2]*START-TEA and RCE-TEA, Institute of Atmospheric Physics, Chinese Academy of Sciences, Beijing* 100029

[3]*School of Geography, Beijing Normal University, Beijing* 100875

(Received 12 January 2009; revised 15 April 2009)

ABSTRACT

Using the regional terrestrial Net Primary Production (NPP) from different observations and models over China, we validated the NPP simulations and explored the relationship between NPP and climate variation at interannual and decadal scales in the Modified Sheffield Dynamic Global Vegetation Model (M-SDGVM) during 1981–2000. M-SDGVM shows agreement with the NPP data from 743 sites under the Global Primary Production Data Initiative (GPPDI). The spatial and the zonal averaged NPP of M-SDGVM agree well with different historic datasets and are closest to the IGBP NPP. Compared to the 1980s, NPP in the 1990s increases in most of China with a high degree of spatial heterogeneity. The multi-year mean NPP of forest types is reasonably modeled (above 500 g C m^{-2} yr^{-1}) while that of C_3 path of photosynthesis (C_3) grasslands is underestimated. The NPP of 7 M-SDGVM main plant functional types (PFTs) increases and the increment of the broad-leaved deciduous forest is the most obvious (5.05 g C m^{-2} yr^{-1}). During the studied period, the annual NPP of M-SDGVM over China increases, with significant fluctuations, at an average rate of 0.0164 Gt C yr^{-1}. Regulated by annual temperature and precipitation, the interannual variation of the total NPP shows more significant correlation with temperature (relativity and probability are R= 0.61, P = 0.00403) than precipitation (R = 0.40, P = 0.08352). CO_2 fertilization may play a key role in the increase of terrestrial ecosystem NPP over continental China, and CO_2 stimulation increases with CO_2 concentrations, and also with the climate variability of the 1980s and 1990s.

Key words: Net Primary Production, dynamic global vegetation model, China

Citation: Mao, J. F., L. Dan, B. Wang, and Y. J. Dai, 2010: Simulation and evaluation of terrestrial ecosystem NPP with M-SDGVM over continental China. *Adv. Atmos. Sci.*, **27**(2), 427–442, doi: 10.1007/s00376–009-9006–6.

1. Introduction

Net Primary Production (NPP) is the rate at which vegetation in an ecosystem fixes CO_2 from the atmosphere (gross primary productivity, GPP) minus the rate at which the vegetation returns CO_2 to the atmosphere through plant respiration (Melillo et al., 1993). As a principal indicator of ecosystem health, resource utilization, and biospheric carbon fluxes, NPP is of great importance to ecological studies, natural resource management, and estimates of the terrestrial carbon sink (Field et al., 1998; Cramer et al., 1999; Potter et al., 2003). Temporal and spatial patterns of terrestrial NPP are expected to change in response to human-induced alterations of climatic conditions, CO_2 concentration, and other factors (Ramankutty and Foley, 1999; McGuire et al., 2001; Nemani et al., 2003; Houghton, 2003). Consequently, accurate estimate of NPP can provide insight into the processes of carbon dynamics within the atmosphere-vegetation-soil continuum and the response of terrestrial ecosystem to future climate change (Jiang et al., 1999; Fang et al., 2003; Cao et al., 2005). NPP varies geographically over time, and it cannot be observed directly at re-

*Corresponding author: MAO Jiafu, jiafumao@yahoo.com.cn

gional and global scales. Nowadays, land ecosystem models with different complexity are widely used to estimate regional and global NPP due to the difficulty in directly measuring NPP at such spatial scales (Tian et al., 1999; Fang et al., 2001; Cao et al., 2003; Dan et al., 2007). The land ecosystem model used here was developed based on eco-physiological, biophysical, and biogeochemical mechanisms, and is driven with actual changes in environmental conditions and ecosystem patterns (such as climate, vegetation, soil, and human activity) (Cramer et al., 1999; Cao et al., 2003). Therefore, it can realistically capture the land ecosystem state pattern at different temporal and spatial scales. More importantly, as one of essential tools in global change research, the land ecosystem model can be directly or indirectly coupled with a climate system model to simulate palaeoclimatology, the ancient ecology and interaction between the terrestrial ecosystem, and the projected climate system under global and regional climatic change (Foley et al., 1996; Friedlingstein et al., 2006). Located in the eastern monsoon region of Eurasia, China occupies approximately 1/15th of the world land area, with climate zones ranging from tropical to subtropical, and with temperate and cold temperate zones, as well as a variety of humid, semi humid, semi-arid, and arid zones. The climatic variability, topographic complexity, natural ecosystem diversity, as well as prevalence of human disturbances mean that China plays an important role in the global carbon cycle, to which it has a large contribution (Fu, 1995; Fang et al., 1996a, b; Piao et al., 2005). In recent years, many studies with different types of land ecosystem models have been implemented for NPP simulations over continental China, and great progress has been made in the study of the terrestrial ecosystem productivity, carbon storage, and carbon fluxes (Xiao et al., 1998; Sun and Zhu, 2001; Piao et al., 2001; Tao et al., 2003; Li et al., 2004; Huang, 2005; He et al., 2005; Dan et al., 2007; Feng et al., 2007; Zhou et al., 2008). However, due to differences between models in parameterization, environmental drivers, vegetation classifications, and the understanding of biological processes, there remains uncertainty in the NPP estimation on the country scale. Additionally, much work still needs to be carried out at the spatial scale ranging from some sites and local plots to the entire country for some ecosystem types for model validation of NPP (Zheng et al., 2003; Dan et al., 2007). Thus, in this paper, we used observed and modeled NPP to assess how well the newly developed M-SDGVM (Mao et al., 2007; 2009) performs over continental China driven with climate forcing and atmospheric CO_2 during the period 1981–2000. We also investigate the interannual and decadal variations of terrestrial NPP over China, and their correlations with climate variability.

2. Methods

2.1 *Model description*

M-SDGVM can simulate carbon and water dynamics and their potential responses to the atmosphere using input data of climate, soil properties, and atmospheric CO_2 in an integrated system. It is an updated version of the standard Sheffield Dynamic Global Vegetation Model (SDGVM) (Woodward et al., 1995, 2004) and primarily designed for the Chinese terrestrial ecosystems (Mao et al., 2007, 2009). Like the module structure of the standard SDGVM (Fig. 1), M-SDGVM incorporates five main modules. The phenology module (PHENOLOGY) defines the vegetation leaf area index and the vegetation phenology. The hydrology module (HYDROLOGY) simulates canopy interception of rainfall, evapotranspiration of the vegetation, bare soil evaporation, snow sublimation, and the groundwater cycle. The soil carbon and nitrogen dynamic module (CENTURY) is based on the well-known Century ecosystem model (Parton et al., 1993). The net primary productivity module (NPP) represents the biogeochemical processes of photosynthesis, the dependence of gas exchange on stomatal conductance, the vegetation respiration, and the nitrogen uptake (Woodward et al., 1995). And the growth module (GROWTH) is mainly applied for simulations of vegetation-soil system carbon dynamics. Compared

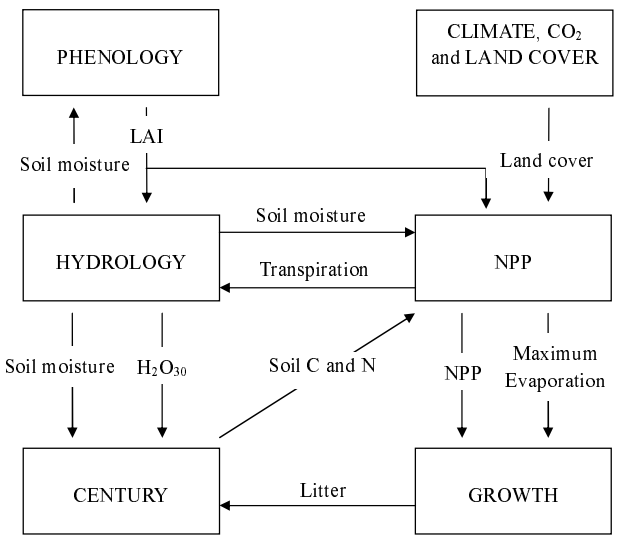

Fig. 1. Schematic of the modules comprising the SDGVM and the connection between sub-models (H_2O_{30} is the H_2O leached below 30 cm; soil C and N represent soil carbon and nitrogen) (Woodward et al., 1995; Woodward and Lomas, 2004).

with the standard SDGVM, the M-SDGVM has some new parameterization schemes including the incorporation of numerical processes related to canopy interception of rainfall (Running and Hunt, 1993), radiation (Sellers et al., 1986; Prentice et al., 1993), root profiles, and soil physical characteristics (Schenk and Jackson, 2002; Dai et al., 2003), and the adoption of a higher resolution vegetation map and soil texture dataset over the continental China (Hou, 1983; Batjes et al., 1997; Huang, 2005). In addition, a few PFT-specific parameters were re-adjusted to ensure realistic simulation of carbon and water balance after these modifications (Mao et al., 2007). Accordingly, in the M-SDGVM, more comprehensive meteorology, vegetation as well as soil information can be used, and more dynamics of the carbon and water of the terrestrial ecosystem, particularly the forest subsystem, can be captured (Mao et al., 2007, 2009).

2.2 *Experimental design*

The M-SDGVM was run with observed data of climate, atmospheric CO_2, soil, and vegetation distribution at a spatial resolution of 0.1° and a time-step of one day. The climate data was derived from the Climate Research Unit (CRU TS 2.1) 20th century climate monthly data set (Mitchell and Jones, 2005) that was used to create daily data, the time resolution of the model, using a simple weather generator in the M-SDGVM. The originally grid precipitation, mean temperature, diurnal temperature range, vapor pressure, and cloud cover with 0.5° resolution were directly converted into 0.1° grid resolution by bilinear interpolation. The calculation of instantaneous downward shortwave radiation and net radiation is derived from Sellers et al. (1986) and Prentice et al. (1993). A dataset of historical global atmospheric CO_2 concentrations extending from 1901 to 2000 was provided by the Carbon Cycle Model Linkage Project (Kicklighter et a., 1999; McGuire et al., 2001). The upper layer (0–30 cm) soil properties are produced from the national soil survey over China (Huang, 2005). Because of the lack of observations, lower-layer (30–100 cm) textures, are based on the hybrid soil texture of global soil data set from the Food and Agriculture Organization (FAO) (Batjes et al., 1997) and the 16-category State Soil Geographic Database (STATSGO) from the U.S. Department of Agriculture. Both layers in the grid are processed at 0.1°×0.1° resolution. The land cover classification at 0.1° grid resolution over China is the potential hybrid vegetation from the vegetation map of China at 1:4 000 000 scale (Hou, 1983) and the Global Vegetation Monitoring Unit (GVM) representing an improvement over global classification schemes available from sensors such as Moderate-resolution

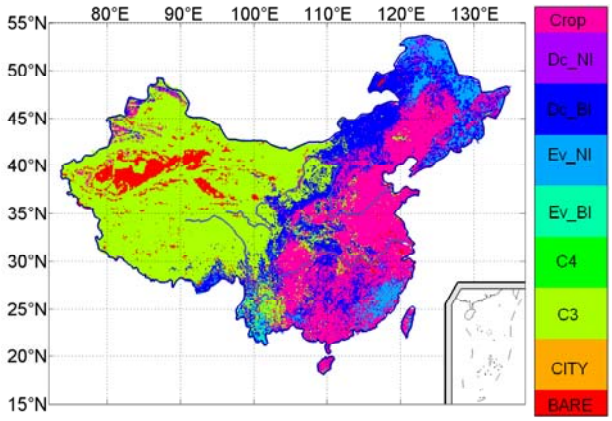

Fig. 2. The dominant potential PFTs' distribution in terms of cover in continental China. Cropland (Crop), needle-leaved deciduous trees (Dc_Nl), broad-leaved deciduous trees (Dc_Bl), needle-leaved evergreen trees (Ev_Nl), broad-leaved evergreen trees (Ev_Bl), grass with C_4 or C_3 photosynthetic path (C_4, C_3), city (CITY), and bare ground (BARE) functional types.

Imaging Spectroradiometer (MODIS) (Huang, 2005). The combined vegetation classification scheme comprises 19 cover types (Huang, 2005), which have been regrouped into 9 plant functional types for this study (Fig. 2).

The M-SDGVM simulation started from a soil defined by texture and depth, climate, vegetation, and atmospheric CO_2 concentration. Therefore, there is a necessary initialization stage in which the carbon and nitrogen storage of the soil is determined (Parton et al., 1993). The model initialization was determined by running with a repeated and random selection of annual climates from 1951 to 1980. Then the model runs until the terrestrial ecosystem is at equilibrium (Net Biome Production is equal to zero), typically after a period of 600 years. When initialization was completed, the M-SDGVM then simulated vegetation with the observed climate and atmospheric CO_2 concentration from 1981 to 2000. At the beginning of each year run of the M-SDGVM, a fraction of ground became available for new growth and the land cover defined in the M-SDGVM input file determined how this new ground was to be allocated between the PFTs.

2.3 *Evaluation data sources*

To assess the accuracy of M-SDGVM forecasts of NPP, we compiled China's NPP data from GPPDI, which is one of the projects in the Ecosystem Model-Data Inter-comparison (EMDI) (Prince et al., 1995; Olson et al., 2001; Zheng et al., 2004). Among the global 7500 validation sites from class A, B, and C, 743 NPP measurement sites in continental China were

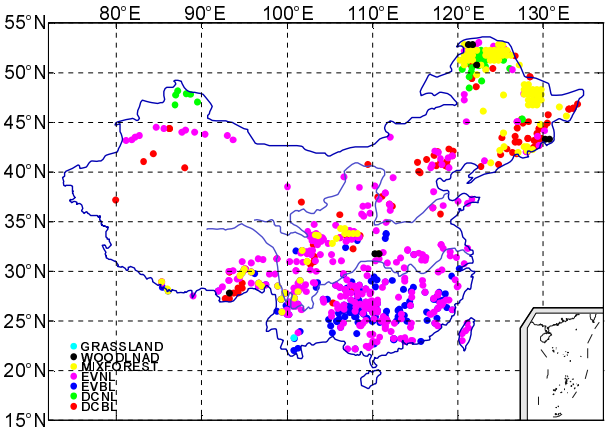

Fig. 3. Distribution of China's 743 NPP sites under GPPDI. Broad-leaved deciduous forests (DCBL) (122 sites), needle-leaved deciduous forests (DCNL) (29 sites), broad-leaved evergreen forests (EVBL) (157 sites), needle-leaved evergreen forests (EVNL) (328 sites), mixed forests (MIXFOREST) (98 sites), woodlands (WOODLAND) (8 sites), and grassland (GRASSLAND) (1 site).

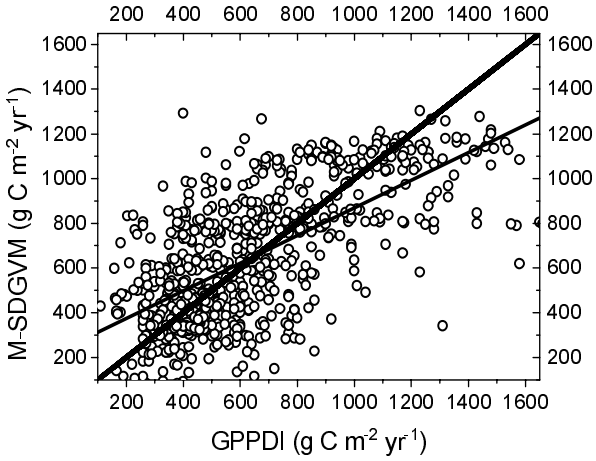

Fig. 4. Comparison between the estimated NPP (g C m^{-2} yr^{-1}) with M-SDGVM and that from the Global Primary Production Data Initiative (GPPDI). The slope of the thick line is 1 and the thin line is the linear fit between the model and observations.

carefully selected for comparison (Fig. 3). The data cover six major forest biomes and one grassland, including broad-leaved deciduous forest (122 sites), needle-leaved deciduous forest (29 sites), broad-leaved evergreen forest (157 sites), needle-leaved evergreen forest (328 sites), mixed forest (98 sites), woodland (8 sites), and grassland (1 site) (Fig. 3). They range across a substantial geographical area, from the sub-boreal Larix forests in northeast and northwest China to tropical rain forests in southern China and on Hainan Island. The elevation of the forest study sites ranges from 10 to 4240 m (mean=1385 m), and stand age from 3 to 350 years (mean=66 years). Total biomass ranges from 3114 to 156 985 g C m^{-2} (mean=18 500 g C m^{-2}), total NPP (above ground plus below ground) from 241 to 4027 g C m^{-2} yr^{-1} (mean=1440 g C m^{-2}), and leaf area index (projected) from 0.17 to 41.78 (mean=8.9) (Luo, 1996; Jiang et al., 1999; Ni, 2001).

Several models' outputs and satellite data including IGBP, GLoPEM, revised GLoPEM, CASA, AVIM-GOALS, and MODIS (Dan et al., 2007) were employed to evaluate the spatial distribution of M-SDGVM NPP during the last 20 years of the last century.

3. Results

3.1 *Evaluation of M-SDGVM NPP with GPPDI dataset in China*

The confidence in terrestrial ecosystem models depends on how well the field data used to develop the model, how well the environmental model driving variables, and how well the model predictions agree with observed data (Zheng et al., 2004). Figure 4 shows the agreement between NPP estimated with M-SDGVM and GPPDI measurements, which demonstrates good performance from M-SDGVM on carbon flux simulation in China's main ecosystem types (R = 0.66, P < 0.00010). In Fig. 5, the simulated and observed variations of NPP from different ecosystem types are schematically illustrated. For many forest ecosystems, the estimated NPP variations, as well as multi-year mean values, corresponds well with the observations. As only 8 woodlands and 1 grassland site could be derived for comparisons, the maximum, mean, and mini-

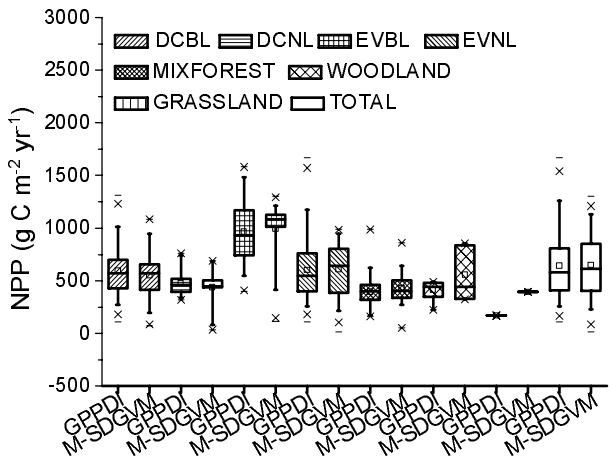

Fig. 5. The maximum, mean, and minimum NPP of individual PFTs and from all PFTs (TOTAL) of 743 NPP sites under GPPDI. Abbreviations and number of PFTs are the same as in Fig. 3.

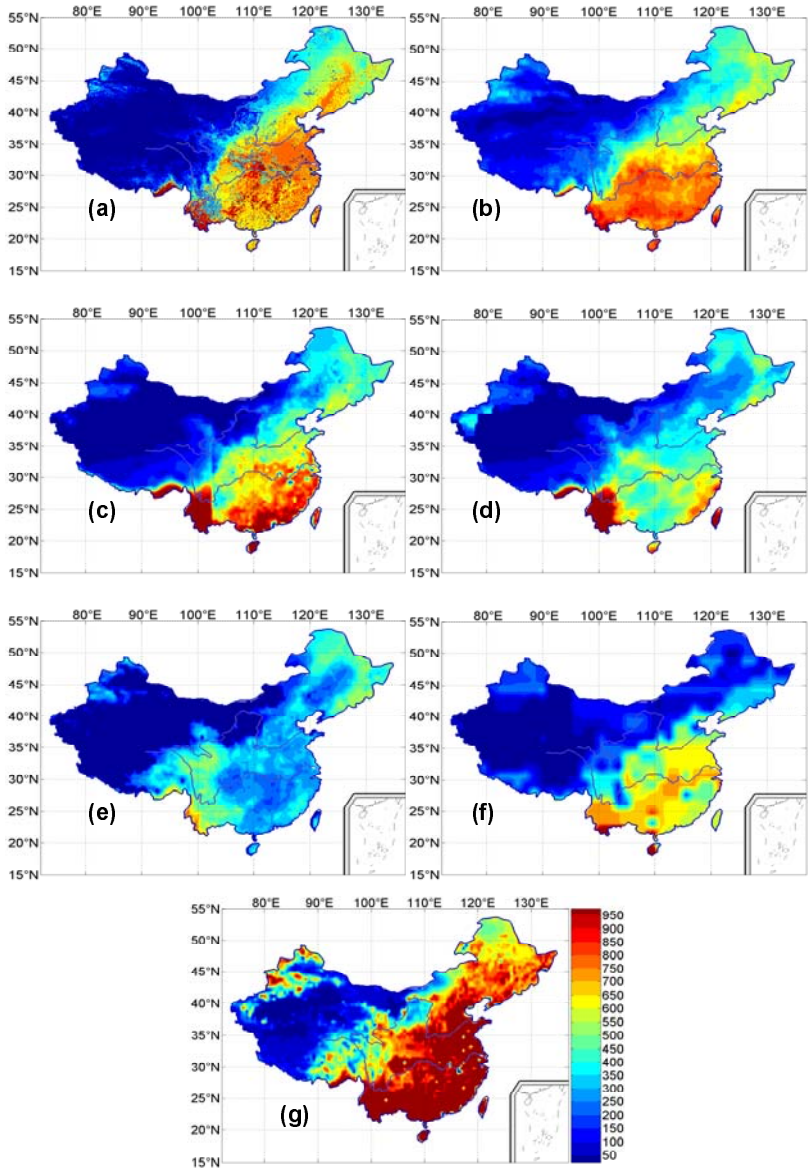

Fig. 6. Annual mean NPP over China from (a) M-SDGVM, (b) IGBP, (c) revised GLoPEM, (d) MODIS, (e) CASA, (f) AVIM-GOALS, and (g) GLoPEM. Units: g C m^{-2} yr^{-1}.

mum NPP of M-SDGVM for these two types were not ideally produced. But under different climatic conditions, M-SDGVM is generally capable to capture the China's main terrestrial NPP, especially in the forest ecosystems, and the estimated multi-year mean as well as variations of NPP corresponds well with the observations. The linear relationship between multi-year mean temperature, precipitation, evapotranspiration, and the M-SDGVM NPP at the 743 sites were also analyzed and the results showed that the modeled NPP correlates well with these variables (all correlation coefficients above 0.8, P <0.0001) (figures not shown here). This indicates that the vegetation carbon fluxes are strongly linked with the water cycles in M-SDGVM and most of the studied sites have high productivities in high temperature and humidity environments.

3.2 *Spatial and temporal simulation of NPP in continental China during* 1981–2000 *in M-SDGVM*

3.2.1 *Spatial simulation and evaluation of M-SDGVM NPP*

Figure 6a shows the simulated spatial distribution of multi-year mean NPP from 1981 to 2000. The average NPP of the estimated 20 years showed that NPP

Table 1. Comparison of area-average and total NPP estimated by M-SDGVM with that from different sources (area of mainland China used in this comparison is 9 520 345 km^2). Relative Error Term (RE) was derived with respect to IGBP NPP Data (The method of calculation for RE is the same as in Dan et al., 2007).

NPP Origin	Area-average over China (units: g C m^{-2} yr^{-1})	Total (units: Gt C)	Relative Error (%)
M-SDGVM	346.517	3.299	−27.26
IGBP	385.373	3.669	0.00
GLoPEM_revised	320.999	3.056	−54.97
MODIS	278.794	2.654	−56.89
CASA	214.188	2.039	−49.95
AVIM-GOALS	268.255	2.554	−37.15
GLoPEM	625.483	5.955	64.89

in southern and eastern China was higher than that in northern and western China, and it increased gradually from the arid land in northwest of the humid areas of southeast China. Dominated by broad-leaved deciduous trees, needle-leaved trees, and broad-leaved evergreen trees (Fig. 2), areas to the southwest of the Yunnan-Guizhou Plateau (centered at 23°N, 102°E), southeast of the Tibetan Plateau (centered at 27°N, 95°E), south of the middle and lower reaches of Yangtze River (centered at 30°N, 115°E), and Changbai Mountains (centered at 43°N, 123°E) produced high NPP rates above 600 g C m^{-2} yr^{-1}. Due to the adequate solar radiation, water, and heat condition, the highest NPP, which was more than 900 g C m^{-2}yr^{-1}, was simulated in the rainforests to the southeast of the Tibetan Plateau. As precipitation in the western arid, semiarid, and grasslands is less than 100 mm yr^{-1}, the simulated NPP in these areas was the lowest and the values range from 0–50 g C m^{-2} yr^{-1}. A large part of the mid-south of the northeast plain (centered at 43°N, 123°E), north China plain, middle and lower reaches of Yangtze River, Sichuan Basin (centered at 30°N, 105°E) and mountainous areas in the south of the Yangtze River are covered with croplands, and the NPP was between 600 and 800 g C m^{-2} yr^{-1}. From the northwestern part of northeast China through the Yellow River loop area (centered at 40°N, 110°E), to the southeast of the Tibetan Plateau, there exists one transitional band, which demonstrates the increase of NPP from the northwest landlocked arid area to the humid southeast part. This area is mainly dominated with C_3 grass, croplands and broad-leaved deciduous tree mosaic (Fig. 2), and the average NPP in this transitional band was around 350 g C m^{-2} yr^{-1}.

In Fig. 6a–g, M-SDGVM and the derived datasets captured the northwest-southeast increasing trend and produced high NPP southeast of the Tibetan Plateau and southwest of the Yunnan-Guizhou Plateau. The area-averaged NPP of M-SDGVM was 346.517 g C m^{-2} and was located in the range of the derived datasets, among which CASA was the lowest (214.188 g C m^{-2}) and GLoPEM was the highest (625.483 g C m^{-2}) (Table 1; Fig. 6a). The spatial distribution of M-SDGVM NPP was the closest to the IGBP mean NPP of 17 models (Fig. 6b) and the relative error was −27.26%, which is the lowest in contrast with other outputs (Table 1). However, for areas covered with croplands, including the northeast plain and Huanghuai plain (centered at 34°N, 115°E), the NPP of M-SDGVM was higher than IGBP and the remote sensing data of MODIS. Along all latitude bands, GLoPEM overestimated NPP, and south of 42°N, except for CASA, all of the modeled and observed results have a similar pattern (Fig. 7). Between 37°N and 42°N, there exists desert, bare soil, C_3 grass, and agriculture land, which has relatively low productivity; thus all simulations and MODIS data produce lower NPP than at other latitudes. Due to the sufficient water, heat, and sunshine, temperate and subtropical areas south of 28°N has higher zonal average NPP than other latitude bands. The northern northeast region was covered by productive broad-leaved deciduous and needle-leaved evergreen trees. Consequently, the zonal average NPP for most of the datasets north of 45°N was relatively high. Due to the bias in simulating tem-

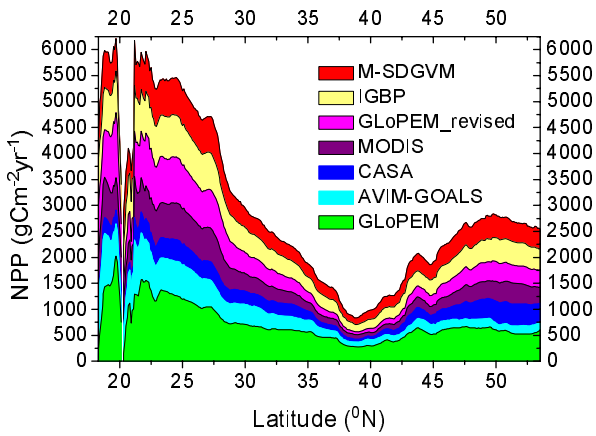

Fig. 7. Zonal average of the annual mean NPP of M-SDGVM, IGBP, GLoPEM revised, MODIS, CASA, AVIM-GOALS, and GLoPEM, units: g C m^{-2} yr^{-1}.

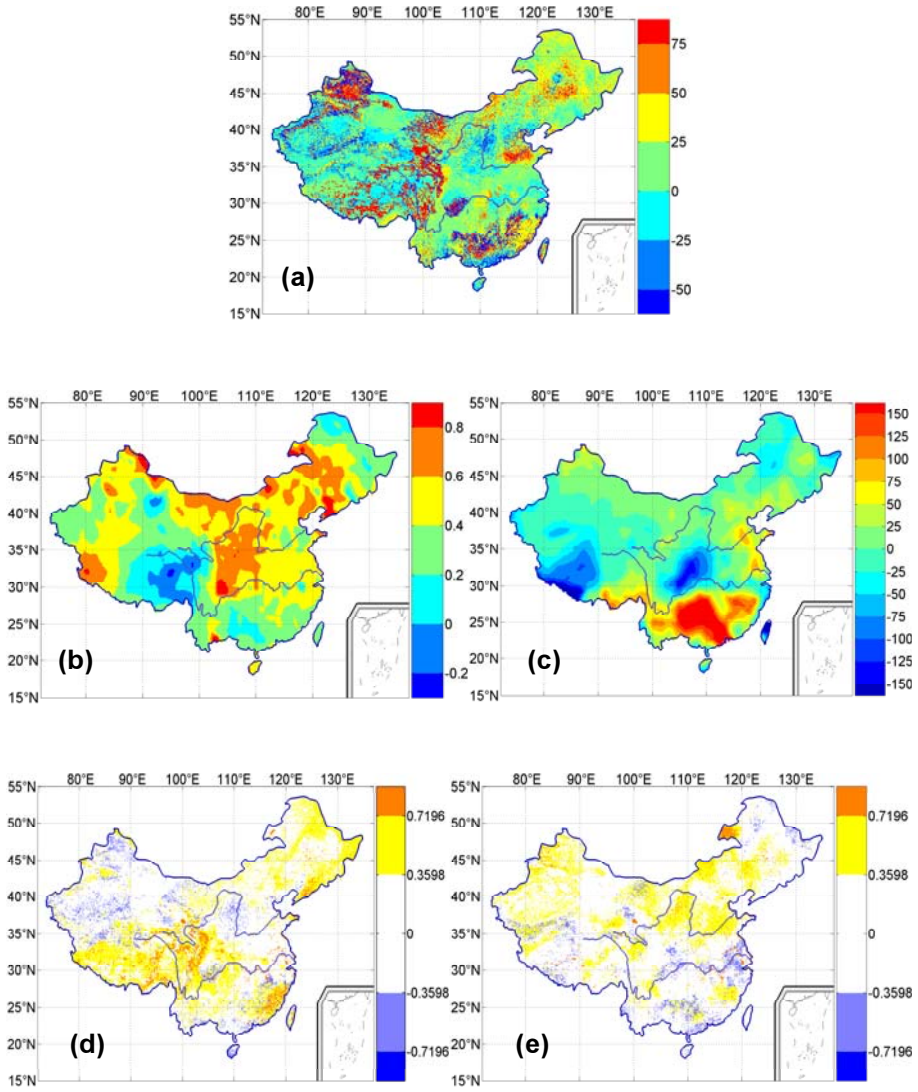

Fig. 8. Difference between annual average (a) M-SDGVM NPP (g C m^{-2}), (b) temperature (°C), and (c) precipitation (mm) over 1991–2000 and over 1981–1990. (d) Correlation coefficient between temperature and NPP, and (e) correlation coefficient between precipitation and NPP during 1981–2000. (Areas with shaded color pass the 90% confidence level).

perature and precipitation in this area, NPP of AVIM-GOALS was underestimated (Dan et al., 2007).

3.2.2 *Ten-year difference of M-SDGVM NPP*

Figure 8a shows the difference of annual average NPP between the two decades of 1991–2000 and 1981–1990. The boreal forests of northeast China (centered at 45°N, 125°E), the Junggar Basin (centered at 45°N, 87°E), the Shandong peninsula (centered at 36°N, 115°E) in the lower reach of the Yellow River, and the needle-leaved evergreen forest in Fujian Province (centered at 26°N, 119°E) have an obvious increase of more than 25 g C m^{-2}. NPP decreases in the south coastal region of Guangdong and Guangxi Provinces (centered at 23°N, 115°E), and in most western regions including the Tarim Basin (centered at 40°N, 85°E), the Yellow River loop area, the central Tibetan Plateau (centered at 32°N, 92°E), and the Sichuan Basin. The most obvious decrease of NPP (more than 25 g C m^{-2}) was found in broad-leaved deciduous forests in the Yellow River loop area, and croplands in the south of Guangdong and Guangxi Provinces. However, due to the impact of microclimate, NPP increases and decreases in continental China were heterogeneous, such as in areas of Tianshan Mountains (centered at 45°N, 85°E), the Tibetan Plateau, and south and northeast of the Sichuan Basin. Except the eastern Tibetan Plateau and the eastern Tarim Basin, temperature in the 1990s

showed an increasing trend in contrast with that in the 1980s (Fig. 8b). In contrast to temperature, the distribution of 10-year increase and decrease of precipitation was more complicated (Figs. 8b, c). South of the Yangtzi River (centered at 25°N, 110°E), a positive precipitation increment was evident (>150 mm in some areas), while southwest of the Tibetan Plateau and in the region between the Qinling Mountains and Daba Mountain (centered at 32°N, 108°E), the decreasing trend of precipitation was marked. In the needle-leaved evergreen forest distributed in southeast Liaoning Province (centered at 40°N, 123°E), to the north of the Sichuan Basin, southwest of the Tibetan Plateau, and in Fujian Province, because of the evident positive changes to temperature (Fig. 8b) and the optimal water and soil wetness conditions, the growing season was extended and the NPP increased greatly (Fig. 8a). The temperature and precipitation in Junggar Basin, the area west of the Yellow River loop area, and the Shandong peninsula in the lower reach of Yellow River increased simultaneously. As a result, the NPP showed an obvious increase (Figs. 9b, c).

Temperature and precipitation are two important external factors that affect and restrict NPP, and hence, spatial correlations of temperature and precipitation with NPP are presented in Figs. 8d and 8e to study their relationship. It is shown in Fig. 8d that positive correlation between temperature and NPP was significant in most areas of the Tibetan Plateau, south of Yangzi River, and in the Northeast. The correlation coefficient east of the Tibetan Plateau was more than 0.7 (passes the 90% confidence level). In arid areas such as the Northwest and the Yellow River loop area, the positive correlation between precipitation and NPP was significant (R >0.30) (Fig. 8e).

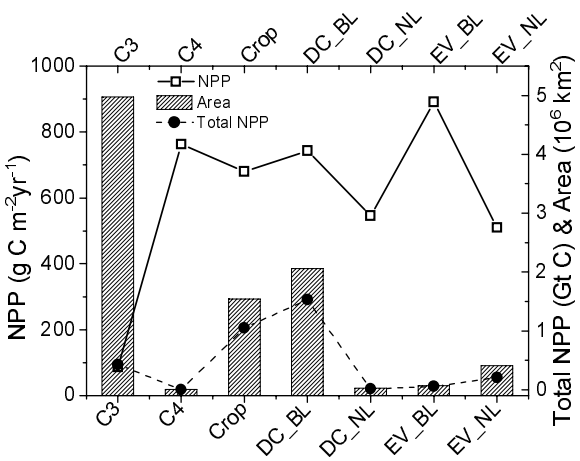

Fig. 9. Estimated multi-year mean NPP (g C m^{-2} yr^{-1}), coverage area (3×10^6 km^2) and total NPP (Gt C) of different PFTs from M-SDGVM during 1981 and 2000.

While to the north of Xiao Hinggan Mountains and Da Hinggan Mountains (centered at 50°N, 123°E), and in the Jianghuai Plain (centered at 32°N, 120°E), the negative correlation between NPP and precipitation was significant (R >0.40, passing the 90% confidence level). In the Yellow River loop area, NPP showed a negative correlation with temperature and a positive correlation with precipitation, which indicated an asynchronous variation of water and heat conditions in contrast with NPP. In this region, the warmer season occurs with less precipitation and drought conditions became serious, which exaggerated water stress on the plants. In south China (centered at 25°N, 110°E), the increase of ten-year averaged precipitation was higher than that from north of Qinling Mountain to Huaihe River (centered at 32°N, 109°E) (Fig. 8c), but the correlations between NPP and precipitation were more significant in the latter than the former (Fig. 8e). Therefore, the contribution of precipitation in north China to NPP was higher than that in the south.

3.2.3 *NPP simulations of different PFTs during* 1981–2000

NPP simulations of M-SDGVM on PFTs over China during the 20 years show that different PFTs had different temporal and spatial variations. The broad-leaved evergreen trees had the largest multi-year mean NPP (891 g C m^{-2} yr^{-1}) while the C_3 grasses had the smallest (87 g C m^{-2} yr^{-1}) (Table 2). Because of differences in coverage areas of different PFTs, total NPP of broad-leaved deciduous forest was the largest (15.3 Gt C) followed by cropland (10.5 Gt C) and C_4 path of photosynthesis (C_4) grassland (0.03 Gt C) (Fig. 9). Comparisons of various PFTs' NPP from M-SDGVM with other derived datasets are presented in Table 2. Adoption of different atmospheric forcings, vegetation classifications, and simulation periods led to outputs from various sources with great discrepancies. Except for the underestimation of C_3 grass NPP (87 g C m^{-2} yr^{-1}), NPP simulated by M-SDGVM for different PFTs were within the ranges of other results and agreed well with observations (Table 2). Figures 10a–g shows the annual anomaly of each PFT's NPP estimated by M-SDGVM. During 1981–2000, variations of different PFTs had different trends, but all PFTs increased with evident annual fluctuations. In comparison to other PFTs, NPP increases were more obvious in broad-leaved deciduous forest (5.05 g C m^{-2} yr^{-1}), needle-leaved deciduous forest (3.53 g C m^{-2} yr^{-1}), broad-leaved evergreen forest (3.53 g C m^{-2} yr^{-1}), and C_4 grassland (3.38 g C m^{-2} yr^{-1}). The largest land average temperature and annual precipitation appeared in 1998 (Fig. 11). In this year, NPP of C_3, C_4 grassland, and needle-

Table 2. Comparison of PFTs' NPP (g C m^{-2} yr^{-1}) estimated by M-SDGVM with that of different sources. Units: g C m^{-2} yr^{-1}, and abbreviations of the PFTs are the same as that in Fig. 2.

NPP Origin	Ev_Nl	Ev_Bl	Dc_Nl	Dc_Bl	C_3	Crop
M-SDGVM	510	891	546	743	87	680
AVIM2[a]	558	801	516	498	28–587	585
CEVSA[b]	515	721	379	515	121–612	648
CASA[c]	354	525	432	304	–	216
Miami[d]	741	810	271	449	220–626	559
Thonthwaite[e]	692	750	350	453	151–584	525
Zhu[f]	367	986	439	643	103–507	427
Luo[g]	439	945	460	548	–	–
Sun[h]	529	971	420	459	116–119	444
Liu[i]	587	945	585	928	271	752
Whittaker[j]	300–1250	300–1250	200–1000	300–1250	125–600	–
Fang[k]	599.4	548.5	587	366.5	–	–
Bunkei[l]	614	1178	614	1178	–	564–690
Observation	179–806[m]	407–1913[m]	179–824[m]	114–1669[m]	230.6±64.9[n]	239–760[o]

Note: a: Huang et al., 2005; b: Tao et al., 2003; c: Piao et al., 2001; d, e, f: Zhu, 2005; g: Luo, 1996; h: Sun et al., 2001; i: Liu, 2001; j: Whittaker and Likens, 1975; k: Fang et al., 1996b; l: Bunkei and Masayuki, 2002; m: Luo, 1996; Ni, 2001; n: Fan et al., 2003; o: Prince et al., 2001.

leaved evergreen forest reached their peak and other PFTs' NPP also showed relatively high values (Fig. 10). In 1994, annual mean temperature and precipitation had high values, and NPP of broad-leaved deciduous forest achieved its largest value (Figs. 11 and 12). In 2000, although annual mean temperature and precipitation were at low levels, NPP of needle-leaved deciduous forests and broad-leaved evergreen forests were simulated to be close to their maximum values, which may be attributed to the high solar radiation in this year (Piao et al., 2001).

3.2.4 *Simulations of annual NPP during* 1981–2000

Figure 11 illustrates annual variations of total precipitation, land averaged temperature, atmospheric CO_2 concentration, and M-SDGVM NPP in continental China during the last 20 years of the 20th century. During 1981–2000, annual NPP in China's terrestrial ecosystem increased and fluctuated with time. It increased from 3.066 Gt C yr^{-1} in 1981 to 3.346 Gt C yr^{-1} in 2000, with an average annual increment of 0.0164 Gt C ($P < 0.0001$). The minimum NPP (3.066 Gt C yr^{-1}) corresponded to the lowest CO_2 concentration, which appeared in 1981, and the maximum NPP (3.522 Gt C yr^{-1}) was accompanied with the highest annual temperature and precipitation, produced in 1998. The appearance time of maximum NPP of M-SDGVM was consistent with that of other complicated models, such as CASA (2.1 Gt C yr^{-1} in 1998) (Piao et al., 2001), CEVSA (3.61 Gt C yr^{-1} in 1998) (Tao et al., 2003), and AVIM2 (3.733 Gt C yr^{-1} in 1998) (Huang, 2005). The multi-year mean NPP of M-SDGVM for 1981–2000 was 3.299 Gt C yr^{-1}, which was close to the values from CEVSA (3.27 Gt C yr^{-1}), AVIM2 (3.445 Gt C yr^{-1}), and the remote sensing model of Zhu (2005) (3.14 Gt C yr^{-1}). Moreover, the multi-year mean NPP of M-SDGVM was closest to the average NPP (3.34 Gt C yr^{-1}) out of the derived datasets in Table 1.

The annual variation and linear trend of total precipitation, average temperature, and atmospheric CO_2 concentration from 1981 to 2000 are shown in Fig. 11. During the 20 years, temperature increased obviously with an annual increment of 0.0517°C (P=4.15×10^{-4}) but precipitation increased only slightly with higher apparent annual variability. The CO_2 concentration went up from 339 ppmv in 1981 to 370.3 ppmv in 2000, with a substantial increment of 1.56 ppmv yr^{-1} (P <0.0001). For further analysis, annual NPP correlated well with annual temperature (R=0.61, P=0.00403), and high temperatures in 1990, 1994 and 1998 were accompanied with high NPP. But, as an exception, there was no high temperature going along with high NPP in 1984. In this year, the annual mean temperature was the lowest in the period 1981–2000, while the solar radiation was the highest out of the in 1980s. Although the annual average temperature was lower than 6.3°C, high summer and autumn temperatures with adequate solar radiation, and the well-distributed precipitation in most areas were advantageous to the ecosystem growth (Piao et al., 2001). In contrast with temperature, correlation between annual precipitation and NPP was not significant (R=0.40, P=0.08352). However, as Fig. 10 shows, annual variations of precipitation regulated and influenced annual NPP greatly, and high

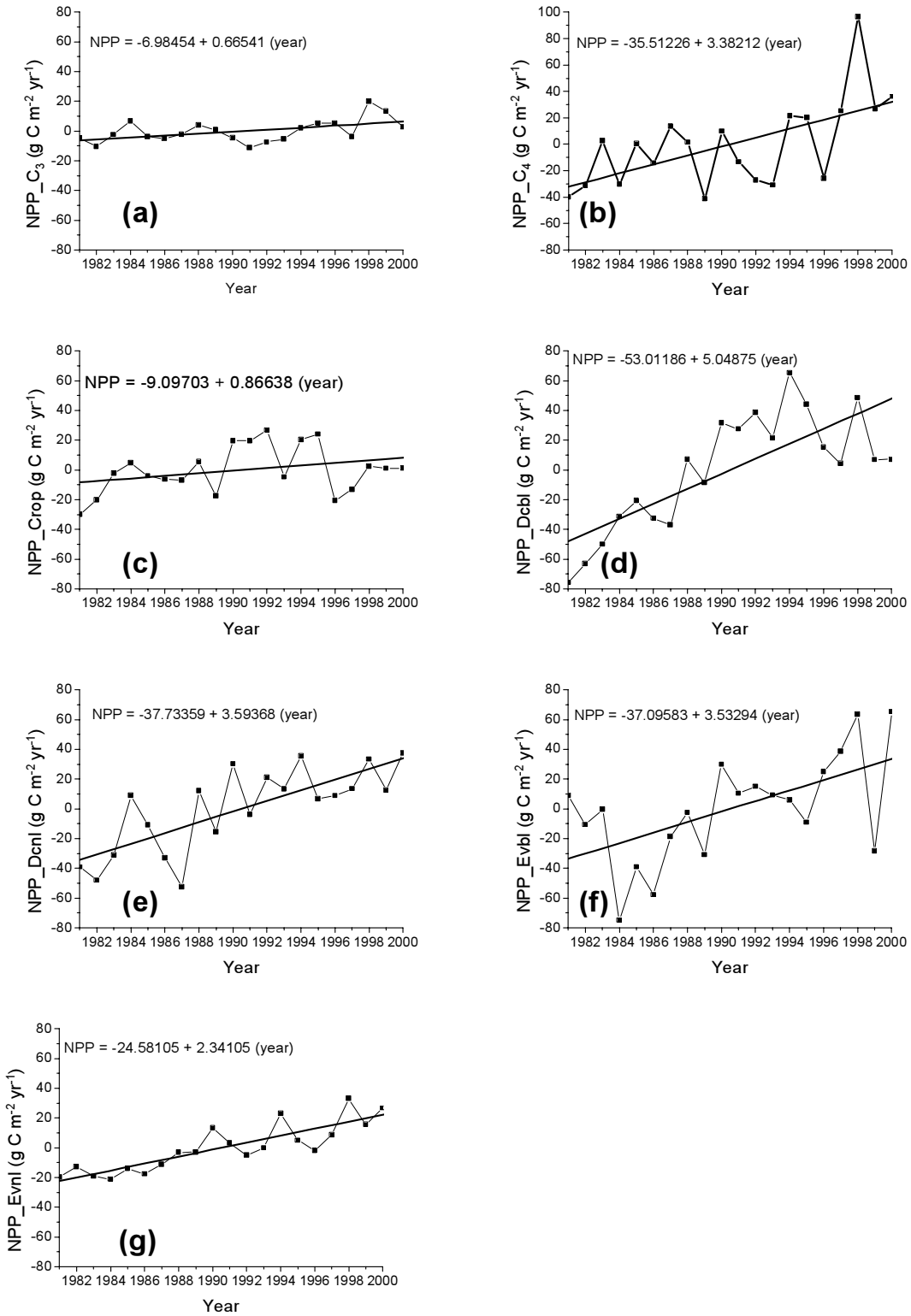

Fig. 10. Annual NPP anomaly of (a) C_3 grass, (b) C_4 grass, (c) Crop land, (d) broad-leaved deciduous tree, (e) needle-leaved deciduous tree, (f) broad-leaved evergreen tree, and (g) needle-leaved evergreen tree regions estimated by M-SDGVM (1981–2000). Units: g C m^{-2} yr^{-1}. The line is a linear fit of the NPP anomaly.

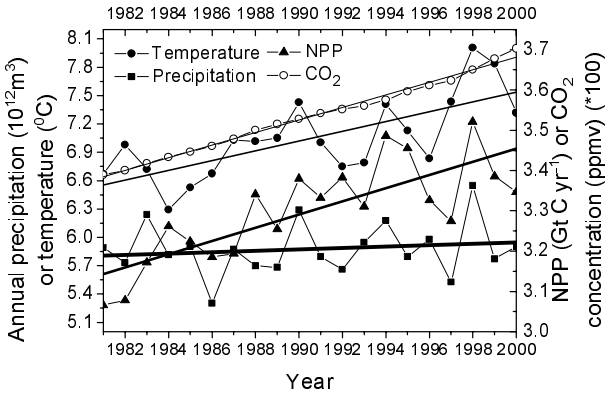

Fig. 11. Annual M-SDGVM total precipitation (10^{12} m^3), temperature (°C) (left axis), NPP (Gt C yr^{-1}), and CO2 concentration (100 ppmv) (right axis) during 1981–2000 over continental China.

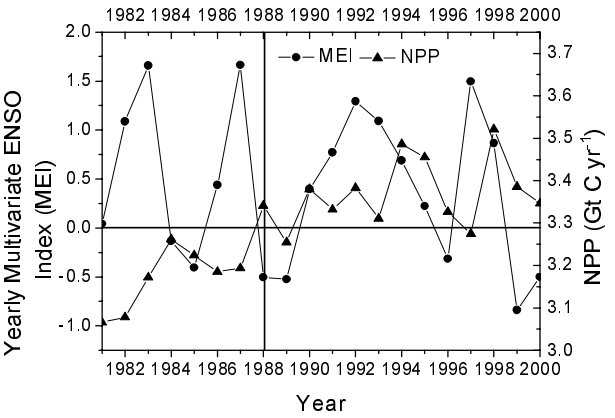

Fig. 12. Yearly Multivariate ENSO Index (MEI) and annual M-SDGVM NPP (Gt C yr^{-1}) during 1981–2000.

NPP in 1990, 1994, and 1998 corresponded with high precipitation and temperature. In 1986, the total precipitation was the lowest in the 20 years (5.3×10^{12} m^3), but as there was more precipitation in spring, total NPP in this year was not the lowest. In 1991, the Mt. Pinatubo eruption in July had noticeable effects on the China's terrestrial NPP. In this year, vegetation production decreased obviously due to reduced temperature, which might have been caused by enhanced stratospheric aerosol above most areas of China (Piao et al., 2001; Lucht et al., 2002).

It is generally accepted that NPP varies with precipitation and temperature changes due to the impacts of ENSO (Lintner, 2002; Jones and Cox, 2005). Much research shows that ENSO has substantial impacts on summer and winter precipitation, and their spatial distributions in China (Jin and Tao, 1999; Cao et al., 2003), and consequently ENSO may influence the variations of annual NPP. China is dominated by a monsoonal climate, which is characterized by seasonal jumps, large interannual variability, and abrupt changes on decadal and longer time scales (Fu, 1995). Monsoon circulations change the distribution and construction of climate elements, and as a result make relationships between ENSO and annual NPP more complicated. Figure 12 shows variations of annual NPP and the multivariate ENSO index (MEI) (http://www.cdc.noaa.gov/people/klaus.wolter/MEI/table.html) (Wolter and Timlin, 1998) between 1981 and 2000. In general, the correlation between MEI and annual NPP was not significant ($R = -0.14$, $P = 0.57000$), but NPP varied with MEI in the opposite phase before 1988 whereas with the same phase after 1988. This might be related with apparent increase of NPP and atmospheric temperature from 1988, as shown in Fig. 11. The annual variation of total NPP in China indicated that NPP decreased to a certain extent in ENSO years like 1986, 1991, and 1993 (Fig. 11). Whereas in ENSO years of 1983, 1990, 1992, 1994, and 1998, reductions of NPP were not remarkable. Especially in 1998, NPP increased to 3.522 Gt C from 3.275 Gt C in 1997, which was the complicated result of different distributions of temperature and precipitation and different responses of the terrestrial ecosystem to ENSO (Tao et al., 2003).

4. Discussions

The multi-year mean distribution of M-SDGVM NPP was closer to the IGBP and MODIS NPP than other results (Figs. 6 and 7). But the simulated cropland NPP of M-SDGVM in the northeast plain area and the Shandong peninsula at the lower reaches of the Yellow River was higher than that from IGBP and MODIS NPP (Fig. 6a, 6b, and 6d). The overestimation of M-SDGVM NPP for croplands can also be found in Table 2, in which M-SDGVM estimated NPP was 680 g C m^{-2} yr^{-1}. Although it was within the range of observational values (239–760 g C m^{-2} yr^{-1}) (Prince et al., 2001), NPP from M-SDGVM was higher than that of other observations or simulation results, which shows that further modification and improvement of M-SDGVM on croplands should be included in future works.

Outputs from M-SDGVM indicated that the decadal climatic change in China alleviated the main climatic constrains to plant growth during the last 20 years of the last century. Some studies have modeled NPP responses to climatic change at regional and larger scales using Normalized Difference Vegetation Index of Advanced Very High Resolution Radiometer (AVHRR NDVI) dataset and pointed out that vegetation activity in the northern middle and high latitudes

has increased over the past two decades (Fang et al., 2003; Nemani et al., 2003; Piao et al., 2005; Zhu, 2005). Zhou et al. (2003) showed that leaf area index (LAI) increased in Eurasia and North America (40°–70°N) respectively from 1982 to 1999. A recent study by Xiao and Moody (2004) indicated an increase in growing season LAI in China between 1982 and 1998. Thus, as a principal indicator of vegetation activity, vegetation NPP in our studies with M-SDGVM in China shows the agreement with trends reported for the northern high latitudes.

Due to differences in geographical positions as well as sensitivities to climatic changes, different PFTs present different temporal and spatial variations (Figs. 9 and 10). Compared to other results, the NPP of C_3 grassland modeled by M-SDGVM was relative low (87 g C m^{-2} yr^{-1}) (Table 2). Still, the model performed well in simulating the NPP of other PFTs, with values within the ranges of various previous research results and observations. Simulations of M-SDGVM indicated that the needle-leaved deciduous forest areas maintained fast growth at a rate of 3.6 g C m^{-2} yr^{-1} (Figs. 10e), which was just lower than that of broad-leaved deciduous forests (5.05 g C m^{-2} yr^{-1}) (Figs. 10d). Needle-leaved deciduous forests are distributed mainly in the northernmost areas of northeast China (Figs. 2 and 3). Due to a heavy forest fire in 1987 and continuous logging, actual NPP increases in needle-leaved deciduous forests may be small (Zhou, 1997; Piao et al., 2005). Since disturbances like fire and human cutting or planting are not included in the current M-SDGVM simulation, NPP growth of the needle-leaved deciduous forests was likely overestimated. Cropland NPP in M-SDGVM had increases of 0.87 g C m^{-2} yr^{-1} under natural conditions (Figs. 10c). There was weak positive correlation ($R = 0.33$, $P = 0.15720$) with statistic annual China's crop yield (http://www.szstv.com/lsj/html/jcck/16082959052.htm), which increased at a rate of 8.249×10^{11} kg yr^{-1} from 1981 to 2000 (figures not shown here). The rapid increase of crop management practices such as fertilization, irrigation, pest control, and resistance undoubtedly enhanced the productivity of crops (Xiao and Moody, 2004). Thus, the weak correlation between annual crop NPP and total crop yield indicates that crop production is not only restricted by natural conditions, but also affected by government policies and the adoption of advanced agricultural science and technology, which shows the implications of the significant influence of human activities on the net primary production of natural terrestrial ecosystems (Imhoff et al., 2004; He et al., 2007).

The increasing NPP from M-SDGVM during 1981 to 2000 may primarily result from the continuing rise of CO_2, which is the so-called CO_2 fertilization effect (Fig. 11). Using the same version of M-SDGVM but with 0.5 degree grid resolution, we conducted a sensitivity experiment of carbon storage in continental China to climatic change and CO_2 change during 1901 to 2000 (Mao et al., 2009). In this experiment, with historical temperature and precipitation variability (0.5° CRU data, Mitchell and Jones, 2005) and constant CO_2 concentration (using the value of 296.3 ppmv from 1900), the total NPP increased at a speed of 0.0041 Gt C yr^{-1} from 3.237 Gt C in 1981 to 3.391 Gt C in 2000. If using historical temperature, precipitation, and CO_2, the interannual variation of NPP was very similar to the former experiment, but with a more evident annual increase of 0.0142 Gt C yr^{-1} (Figs. 5a, 5d and Figs. 6a, 6d, Mao et al., 2009). These factorial experiments indicate that the CO_2 fertilization may play a key role in the increase of terrestrial ecosystem NPP in continental China, and especially shows that the CO_2 stimulation increased with CO_2 concentrations and also with the climate variability of the 1980s and 1990s. According to Cao et al. (2004), the warming trend particularly enhanced NPP in northern high latitudes, and increases in precipitation helped to enhance NPP in the northern middle latitudes and the tropics, with increases in atmospheric CO_2 contributing to NPP increases in all regions. In our simulation, over the whole of continental China, the evident CO_2 fertilization accompanied with significant correlation between annual temperature and NPP indicates that the CO_2 fertilization effect on total NPP is expected to increase in warm environments. And this is also consistent with studies suggesting that the response of photosynthetic biochemical reactions to increases in atmospheric CO_2 is higher under warmer conditions (Kirschbaum et al., 1994; Cao et al., 2004).

The interannual variation of total NPP modeled by M-SDGVM was correlated more significantly with temperature than precipitation, which demonstrated the agreement between the increasing trend of annual NPP and temperature in the last two decades of the 20th century. This is consistent with previous investigations that show productivity in northern high latitudes increasing in response to elevated temperatures, especially during spring (Tucker et al., 2001, Lucht et al., 2002; Zhou et al., 2003; Xiao and Moody, 2004). The evident correlation between temperature and NPP was also indicated in previous work (e.g., Cui et al., 2005) which studied variations of NPP in different seasons during 1981 to 2000 using the GLoPEM and observational data such as temperature, precipitation, and land use changes. Cui et al. (2005) concluded that seasonal mean NPP, temperature, and precipitation changed greatly during the 20 years and the inter-

annual variation of the seasonal NPP was consistent with that of the seasonal mean temperature, but not with seasonal precipitation.

The inter-annual variation of M-SDGVM NPP had no significant correlation with the MEI ($R = -0.14$, $P = 0.57000$). Globally, in general, NPP decreases in El Niño seasons and increases in La Niña seasons; however, the response varies widely in individual ENSO events and in different regions (Lintner, 2002; Cao et al., 2004). China has very complicated topography and the climate is dominated by summer monsoon circulations which have variable effects on NPP. The El Niños in the years 1994 and 1998 was comparatively week. (Fig. 12). As a result, temperature and precipitation were relatively high in these two years (Fig. 11). Especially in 1998, the total precipitation was the highest in the 20 years and mean temperature was the highest in the past 100 years. During these two years, increasese of precipitation in spring and summer were obvious and in most of continental China the annual precipitation was more than average (Tao et al., 2003). The sufficient precipitation plus the continuously high temperature in spring helped the accumulation of NPP. Consequently, both M-SDGVM and the remote sensing model from Zhu (2005) produced the highest two NPP values in 1994 and 1998 during the last 20 years of the last century. Moreover, all of M-SDGVM, CASA, CEVSA, and AVIM2 simulated the highest NPP values in 1998 out of the period 1981–2000. It is interesting that the maximum NPP in the remote sensing model from Zhu (2005) appeared in 1994 and not in 1998, and the second highest NPP values were not simulated in 1994 by the process-based CEVSA and AVIM2 models. In addition, the NPP modeled by M-SDGVM and CASA was more correlative with temperature (in CASA, $R = 0.72$, $P = 0.00100$) than precipitation, while the annual NPP of CEVSA correlated significantly with precipitation but not temperature. The influence of the climatic anomaly caused by ENSO on annual NPP is complicated. And because of differences in parameterization and driving factors like climate, vegetation, and soil, different ecosystem models differ greatly in NPP simulations in ENSO years. Therefore, extensive simulations and evaluations of NPP remain a challenge for further studies as the mechanism of NPP variations is explored and modification and development of ecosystem models continues.

5. Conclusions

Using the inventory, satellite data, and modeled outputs, we estimated and evaluated the multi-year mean, interannual, and decadal differences of NPP modeled by the M-SDGVM at different spatial scales during 1981 to 2000 in continental China. Based on the data comparison, we analyzed and investigated correlations of temporal and spatial variations of NPP with different climate factors. Key conclusions are:

(1) M-SDGVM showed good performance of NPP on different temporal and spatial scales, which indicates that M-SDGM has great potential in capturing NPP of main terrestrial ecosystems under different climatic conditions of China.

(2) Compared to the 1980s, terrestrial ecosystem NPP of the 1990s in most of China increased, but the increases and decreases had a high degree of spatial heterogeneity. The decadal changes of temperature, precipitation, and solar radiation during the last 20 years of last century were in the direction of being advantageous to the increase of terrestrial ecosystem NPP.

(3) During 1981 to 2000, both PFTs NPP and annual total NPP of M-SDGVM over China increased, with fluctuations. With the regulation of temperature and precipitation, annual NPP of M-SDGVM had more significant correlation with temperature (R=0.61, P=0.00403) than precipitation (R=0.40, P=0.08352). The CO_2 fertilization effect combined with warm environments contributed to the significant annual increment of terrestrial ecosystem NPP (0.0164 Gt C yr^{-1}, P <0.0001).

During the last 20 years of the last century, China experienced substantial changes in land use and land cover due to its "reform and opening" policies, which may contribute substantially to trends in vegetation activity and NPP (Liu et al., 2005). On the other hand, the interannual variations of seasonal and monthly terrestrial NPP and their possible drivers in China have indicated an important role for exploring how NPP changes and its possible feedbacks (Piao et al., 2005; Cui et al., 2005). Thus, further comprehensive research of NPP over a variety of time scales will facilitate our greater understanding of the rules governing NPP variations and terrestrial carbon cycles over China.

Acknowledgements. The first author is very grateful for help on modifications and applications of SDGVM to Prof. F Ian Woodward and Dr. Mark Lomas from Sheffield University, U.K. The first author would also like to give thanks to the comments of Prof. Andy Pitman from the University of New South Wales, Australia. This paper is partly supported by the China Meteorological Administration through Grant GYHY (QX) 2007-25, the 973 project under Grant 2005CB321703, the Fund for Innovative Research Groups under Grant No. 40821092, and the National Natural Science Foundation of China (NSFC)

project under Grant Nos. 40225013 and 40730106.

REFERENCES

Batjes, N. H., G. Fisher, F. O. Nachtergaele, V. S. Stolbovoy, and H. T. van Velthuizen, 1997: *Soil Data Derived from WISE for Uses in Regional and Global AEZ Studies* (*Version* 1.0). FAO/IIASA/ISRIC, Laxenburg, 27pp.

Bunkei, M., and T. Masayuki, 2002: Integrating remotely sensed data with an ecosystem model to estimate net primary productivity in East Asia. *Remote Sens. Environ.*, **81**, 58–66.

Cao, M. K., D. P. Stephen, K. R. Li, B. Tao, J. Small, and X. Shao, 2003: Response of terrestrial carbon uptake to climate interannual variability in China. *Global Change Biology*, **9**, 536–546.

Cao, M. K., S. D. Prince, J. Small, and S. J. Coetz, 2004: Remotely sensed interannual variations and trends in terrestrial net primary productivity 1981–2000. *Ecosystems*, **7**, 233–242.

Cao, M. K., S. D. Prince, B. Tao, J. Small, and K. R. Li, 2005: Regional pattern and interannual variations in global terrestrial carbon uptake in response to changes in climate and atmospheric CO_2. *Tellus* (*B*), **57**, 210–217.

Cramer, W., and Coauthors, 1999: Comparing global models of terrestrial net primary productivity (NPP): Overview and key results. *Global Change Biology*, **5**(Suppl. **1**), 1–15.

Cui, L. L, J. Shi, P. Tang, and Z. Q. Gao, 2005: Seasonal change of terrestrial net primary productivity in China. *Progress in Geography*, **24**(3), 8–17.

Dai, Y., and Coauthors, 2003: The common Land Model (CLM). *Bull. Amer. Meter. Soc.*, **84**, 1013–1023.

Dan, L., J. Ji, and Y. He, 2007: Use of ISLSCP II data to intercompare and validate the terrestrial net primary production in a land surface model coupled to a general circulation model. *J. Geophys. Res.*, **112**, D02S90, doi: 10.1029/2006JD007721.

Fan, J. W., H. P. Zhong, B. Liang, P. L. Shi, and G. R. Yu, 2003: Carbon stock in grassland ecosystem and its affecting factors. *Journal of Grassland*, **25**(6), 51–58.

Fang, J. Y., G. H. Liu, and S. L. Xu, 1996a: Carbon cycle of terrestrial ecosystems in China and its global significance. *Hot Spots in Modern Ecology*, Wang et al., Eds., China Science and Technology Press, Beijing, 24–250. (in Chinese)

Fang, J. Y., G. H. Liu, and S. L. Xu, 1996b: Carbon pools in terrestrial ecosystems in China. *Hot Spots in Moden Ecology*, Wang et al., Eds., China Science and Technology Press, Beijing, 251–277. (in Chinese)

Fang, J. Y., S. L. Piao, Z. Y. Tang, C. H. Peng, and W. Ji, 2001: Interannual variability in netprimary productivity and precipitation. *Science*, **293**, 17234.

Fang, J. Y., S. L. Piao, J. S. He, and W. H. Ma, 2003: Increasing net primary production in China from 1982 to 1999. *Frontiers in Ecology and the Environment*, **1**(6), 293–297.

Feng, X, G. Liu, J. M. Chen, M. Chen, J. Liu, W. M. Ju, R. Sun, and W. Zhou, 2007: Net primary productivity of China's terrestrial ecosystems from a process model driven by remote sensing. *Journal of Environmental Management*, **85**(3), 563–573.

Field, C. B., M. J. Behrenfeld, J. T. Randerson, and P. Falkowski, 1998: Primary production ofthe biosphere: Integrating terrestrial and oceanic components. *Science*, **281**, 237–240.

Foley, J. A., I. C. Prentice, N. Ramankutty, S. Levis, D. Pollard, S. Sitch, and A. Haxeltine, 1996: An integrated biosphere model of land surface processes, terrestrial carbon balance, and vegetation dynamics. *Global Change Biology*, **4**, 561–579.

Friedlingstein, P., and Coauthors, 2006: Climate-carbon cycle feedback analysis: Results from the C4MIP model intercomparison. *J. Climate*, **19**, 3337–3353.

Fu, C., 1995: Dynamics of monsoon-driven ecosystem: Concept, preliminary evidence and proposal for further research. *China Contributions to Global Change Studies*, Ye et al., Eds., Science Press, Beijing, 103–106. (in Chinese)

He, Y., L. Dan, W. J. Dong, J. J. Ji, and D. H. Qin, 2005: The terrestrial NPP simulations in China since Last Glacial Maximum. *Chinese Science Bulletin*, **50**, 2074–2079. (in Chinese)

He, Y., W. J. Dong, X. Q. Guo, and J. J. Ji, 2007: The Chinese terrestrial NPP simulation from 1971 to 2000. *Journal of Glaciology and Geocryology*, **29**(2), 226–232.

Hou, H. Y., 1983: Vegetation map of China, 1:14000000. *Annals of the Missouri Botanical Garden*, **70**(3), 509–548.

Houghton, R. A., 2003: Revised estimates of the annual net flux of carbon to the atmosphere from changes in land use and land management 1850–2000. *Tellus*, **55B**(2), 378–390.

Huang, M., 2005: The simulations of water, heat and carbon cycle in the ecosystem of continental China. Ph. D. dissertation, Institute of Geographic Sciences and Natural Resources Research, Chinese Academy of Sciences, Beijing, China, 137pp. (in Chinese)

Imhoff, M. L., L. Bounoua, T. Ricketts, C. Loucks, R. Harriss, and W. T. Lawrence, 2004: Global patterns in human consumption of net primary production. *Nature*, **429**(6994), 870–873.

Jiang, H., M. J. Apps, Y. L. Zhang, C. H. Peng, and P. M. Woodare, 1999: Modelling the spatial pattern of net primary productivity in Chinese forests. *Ecological Modelling,* **122**, 275–288.

Jin, Z. H., and S. Y. Tao, 1999: A study on the relationship between ENSO cycle and rainfalls during summer and winter in eastern China. *Chinese J. Atmos. Sci.*, **23**, 663–672. (in Chinese)

Jones, C. D., and P. M. Cox, 2005: On the significance of atmospheric CO_2 growth rate anomalies in 2002–2003. *Geophys. Res. Lett.*, **32**, L14816, doi: 10.1029/2005GL023027.

Kichlighter, D. W., and Coauthors, 1999: A first-order analysis of the potential role of the potential role of CO_2 fertilization to affect the global carbon budget: A comparison of four terrestrial biosphere models. *Tellus*, **51B**, 343–366.

Kirschbaum, M. U. F., and Coauthors, 1994: Modelling forest response to increasing CO_2 concentration under nutrient-limited conditions. *Plant, Cell and Environment,* **17**(10), 1081–1099.

Li, K. R., S. Q. Wang, and M. K. Cao, 2004: Vegetation and soil carbon storage in China. *Science in China* (*D*), **47**(1), 49–57.

Lintner, B.R., 2002: Characterizing global CO_2 interannual variability with empirical orthogonal function/principal component (EOF/PC) analysis. *Geophys. Res. Lett.*, **29(19)**, 1921, doi: 10.1029/2001GL014419.

Liu, M. L., 2001: Research of land use/land cover change and terrestrial ecosystem vegetation carbon and production over China. Ph. D. dissertation, Institute of Remote Sensing Applications, Chinese Academy of Sciences, Beijing, China. (in Chinese)

Liu, J., H. Tian, M. Liu, D. Zhuang, J. Melillo, and Z. Zhang, 2005: China's changing landscape during the 1990s: Large-scale land transformation estimated with satellite data. *Geophys. Res. Lett.*, **32**, L02405, doi: 10.1029/2004GL021649.

Lucht, W., and Coauthors, 2002: Climatic control of the high-latitude vegetation greening trend and Pinatubo effect. *Science*, **296**(5573), 1687–1689.

Luo, T. X.,1996: Patterns of biological production and its mathematical models for main forest types of China. Ph. D. dissertation, Committee of Synthesis Investigation of Natural Resources, Chinese Academy of Sciences, Beijing, China, 211pp. (in Chinese)

Mao, J. F., B. Wang, Y. Dai, F. I. Woodward, P. J. Hanson, and M. K. Lomas, 2007: Improvements of a dynamic global vegetation model and simulations of carbon and water at an up-land oak forest. *Adv. Atmos. Sci.*, **24**(2), 311–322, doi: 10.1007/s00376-007-0311-7.

Mao, J. F., B. Wang, and Y. Dai, 2009: Sensitivity of the carbon storage of potential vegetation to historical climate variability and CO_2 in the continental China. *Adv. Atmos. Sci.,* **26**(1), 87–100.

McGuire, A. D., and Coauthors, 2001: Carbon balance of the terrestrial biosphere in the twentieth century: analyses of CO_2, climate and land use effects with four process-based ecosystem models. *Global Biogeochemical Cycles*, **15**, 183–206.

Melillo, J. M., A. D. McGuire, D. W. Kicklighter, B. Moore, C. J. Vorosmarty, and A. L. Schloss, 1993: Global climate change and terrestrial net primary production. *Nature*, **363**, 234–240.

Mitchell, T. D., and P. D. Jones., 2005: An improved method of constructing a database of monthly climate observations and associated high-resolution grids. *International International Journal of Climatology*, **25(6)**, 693–712.

Nemani, R. R., C. D. Keeling, H. Hashimoto, W. M. Jolly, S. C. Piper, C. J. Tucker, R. B. Myneni and S. W. Running, 2003: Climate-driven increases in global terrestrial net primary production from 1982 to 1999. *Science*, **300**, 1560–1563.

Ni, J., 2001: Carbon storage in terrestrial ecosystems of China: estimates at different spatial resolutions and their responses to climate change. *Climatic Change*, **49**, 339–358.

Olson, R. J., J. M. O. Scurlock, S. D. Prince, D. L. Zheng, and K. R. Johnson, 2001: NPP multi-biome: Global primary production data initiative products. The Oak Ridge National Laboratory Distributed Active Archive Center, Oak Ridge, Tennessee, US. [Available on-line from http://www.daac.ornl.gov/]

Parton, W. J., and Coauthors, 1993: Observations and modeling of biomass and soil organic matter dynamics for the grassland biome worldwide. *Global Biogeochemical Cycles*, **7**, 785–809.

Piao, S., J. Fang, and Q. Guo, 2001: Terrestrial net primary production and its spatio-temporal patterns in China during 1982–1999. *Acta Scientiaram Naturalium Uriversitatis Pekinertsi*, **37(4)**, 563–569. (in Chinese)

Piao, S., J. Fang, L. Zhou, B. Zhu, K. Tan, and S. Tao, 2005: Changes in vegetation net primary productivity from 1982 to 1999 in China. *Global Biogeochem. Cycles*, **19**, GB2027, doi: 10.1029/2004GB002274.

Potter, C. S., S. A. Klooster, R. Myneni, V. Genovese, P.-N. Tan, and V. Kumar, 2003: Continental-scale comparisons of terrestrial carbon sinks estimated from satellite data and ecosystem modeling 1982–1998. *Global Planet Change*, **39**, 201–213.

Prentice, I. C., M. T. Sykes, and W. Cramer, 1993: A simulation model for the transient effects of climate change on forest landscapes. *Ecological Modelling*, **65**, 51–70.

Prince, S. D., R. J. Olson, G. Dedieu, G. Esser, and W. Cramer, 1995: Global primary production data initiative project description. IGBP-DIS Working Paper No. 12, International Geosphere-Biosphere Program-Data and Information System, Toulouse, 38pp.

Prince, S. D., J. Hasket, M. Steininger, H. Strand, and R. Wright, 2001: Net Primary production of U. S. Midwest croplands from agricultural harvest yield data. *Ecological Applications*, **11**, 1194–1205.

Ramankutty, N., and J. A. Foley, 1999: Estimating historical changes in global land cover: Croplands from 1700 to 1992. *Global Biogeochemical Cycles*, **13**, 997–1028.

Running, S. W., and E. R. Hunt, 1993: Generalization of a forest ecosystem process model for other biomes, BIOME-BGC and an application for global-scale models. *Scaling Physiological Processes: Leaf to Globe*, J. R. Ehleringer and C. B. Field, Eds., Academic Press, Inc, New York, 141–158.

Schenk, H. J., and R. B. Jackson, 2002: The global biogeography of roots. *Ecological Monagraph*, **72**(3),

311–328.

Sellers, P. J., Y. Mintz, Y. C. Sud, and A. Dalcher, 1986: A simple biosphere model (SIB) for use within general circulation models. *J. Atmos. Sci.*, **43**, 505–531.

Sun, R., and Q. J. Zhu, 2001: Estimation of net primary productivity in China using remote sensing data. *Journal of Geographical Sciences*, **11**, 14–23.

Tao, B., K. R. Li, and X. M. Shao, 2003: Temporal and spatial patterns of net primary production of terrestrial ecosystems in China. *Acta Geographica Sinaca*, **58**(3), 372–380. (in Chinese)

Tian, H., J. M. Mellillo, D. W. Kicklighter, A. D. McGuire, and J. V. K. Helfrich, 1999: The sensitivity of terrestrial carbon storage to historical climate variability and atmospheric CO_2 in the United States. *Telles*, **51B**, 414–452.

Tucker, C. J., D. Slayback, J. E. Pinzon, S. O. Los, R. B. Myneni, and M. G. Taylor, 2001: Higher northern latitude NDVI and growing season trends from 1982 to 1999. *Int. J. Biometeorol.*, **45**, 184–190.

Whittaker, R. H., G. E. Likens, 1975: The biosphere and man. *Primary Productivity of the Biosphere*, H. Lieth and R. H. Whittaker, Eds., Springer-Verlag, New York, 305–328.

Wolter, K., and M. S. Timlin, 1998: Measuring the strength of ENSO events—how does 1997/98 rank? *Weather*, **53**, 315–324.

Woodward, F. I., and M. R. Lomas, 2004: Vegetation dynamics-simulation responses to climatic change. *Biological Reviews*, **79**, 643–670.

Woodward, F. I., T. M. Smith, and W. R. Emanuel, 1995: A global primary productivity and phytogeography model. *Global Biogeochemical Cycles*, **9**, 471–490.

Xiao, X., J. M. Melillo, D. W. Kicklighter, Y. Pan, A. D. McGuire, and J. Helfrich, 1998: Primary production of terrestrial ecosystems in China and its equilibrium responses to changes in climate and atmospheric CO_2 concentration. *Acta Phytoecologica Sinica*, **22**, 97–118.

Xiao, J., and A. Moody, 2004: Trends in vegetation activity and their climatic correlates: China 1982 to 1998. *Int. J. Remote Sens.*, **25**(24), 5669–5689.

Zheng, D. L., S. Prince, and R. Wright, 2003: Terrestrial net primary production estimates for 0.5° grid cells from field observations—A contribution to global biogeochemical modeling. *Global Change Biology,* **9**, 46–64.

Zheng, D. L., S. D. Prince, and R. Wright, 2004: NPP multi-biome: Gridded estimates for selected regions worldwide, 1989–2001, revision 2. The Oak Ridge National Laboratory Distributed Active Archive Center. Oak Ridge, Tennessee, US. [Available on-line from http://www.daac.ornl.gov/]

Zhou, G. S., W. P. Yuan, L. Zhou, and Y. R. Zheng, 2008: Terrestrial ecosystem productivity and carrying capacity in northeast China. *Journal of Plant Ecology*, **32**(1), 65–72.

Zhou, L., R. K. Kaufmann, Y. Tian, R. B. Myneni, and C. J. Tucker, 2003: Relation between interannual variations in satellite measures of northern forest greenness and climate between 1982 and 1999. *J. Geophys. Res.*, **108**(D1), 4004, doi: 10.1029/2002JD002510.

Zhou, Y. L., 1997: *Geography of the Vegetation in Northeast China*. Science Press, Beijing, 289–297. (in Chinese)

Zhu, W. Q., 2005: Estimation of net primary productivity of Chinese terrestrial vegetation based on remote sensing and its relationship with global climate change. Ph. D. dissertation, Beijing Normal University, Beijing, China, 163pp. (in Chinese)